SPACECRAFT STRUCTURAL ANALYSIS TODAY AND YESTERDAY

Charles R. Gamblin, P. E.
Senior Lead Engineer – Structures Group
Teledyne Brown Engineering
Huntsville, Alabama

ABSTRACT

This paper presents a present-day MSC NASTRAN/PATRAN* static/dynamic FEM of the first Saturn I First Stage Booster (1962). This historic Saturn I launch vehicle was successfully flown nineteen times with one manned launch mission (Apollo 7) an 163 earth orbit practice run for the more historic Apollo 11 moon landing thirty years ago in July 1969. The Saturn I FEM shown is a gross static force and dynamic displacement model with limited stress accuracy. More detailed substructured models would be required for a complete stress analysis, which is the standard operating procedure by today's structural analysis methods.

In the yesteryear, the original static analysis approach involved the judicious application of free body cuts through the clustered tank booster assembly to expose the indeterminate internal reaction forces. Each tank was considered as a "finite element" in the stack-up of structural stiffness (matrix) components. Applying the laws of static equilibrium, the formation of the redundant equations resulted in a 12x12 stiffness matrix for solution. This paper shows examples of the original redundant equation formulation and the computer analysis output results in free body format.

* Trademarks are capitalized and listed at the end of this paper.

Introduction

The first NASA Saturn/Apollo launch vehicle had a first stage booster configuration significantly different than that of the Saturn V Apollo vehicle which transported men to the moon first in July 1969. The Saturn I first stage booster (Figure 1) was a clustered tank arrangement of one Jupiter missile liquid propellant tank encircled by eight Redstone missile tanks and powered by eight H-1 engines at 150,000 pounds of thrust each. The Jupiter and Redstone were proven Army ordinance missiles and all the fabrication tooling was available for NASA use at Redstone Arsenal, Alabama in 1960. The original structural analysis described herein was started in May of the same year. Numerous analysis modifications were required to support the design and fabrication of ten Saturn I and IB vehicles. Each vehicle involved different structural configurations, launch weights and flight external load sets.

The first hurdle to overcome for an accurate structural analysis was to determine the internal load distributions among the nine different propellant tanks. This required a matrix solution of a set of redundant internal reaction forces produced by a known set of externally applied loads (Figure 2). It was determined that the booster internal loads were best defined just below the eight leg spider beam assembly at the interface pin attachments to each of the propellant tank's upper ring frames. Of course, by today's structural analysis methods, e.g., MSC/NASTRAN, this is simply a specific set of finite element GRID point forces resulting from a defined set of boundary conditions.

Finite Element Model Idealization

The MSC/NASTRAN and MSC/PATRAN Finite Element Model (Figure 3) of the Saturn I first stage booster is a straight-forward assembly of eleven substructured FEM's:

1	Spider Beam Structure
2	Center 105" Diameter Tank Substructure
3-6	Outer 70" Diameter LOX Tank Substructures
7-10	Outer 70" Diameter Fuel Tank Substructures
11	Thrust Beam Substructure

The 70" diameter tanks differ primarily in minor length and thickness differences and significantly in the upper attachment fixity. The 70" fuel tanks are free to thermally expand at the spider beam attachment; i.e. no axial loads are imposed at the upper end.

The NASTRAN/PATRAN Saturn I clustered tank FEM (Figure 3) contains the following entities:

GRID Points	2,018
QUAD4 Elements	1,832
TRI3 Elements	148
BEAM Elements	120

This degree of element mesh is <u>not</u> refined to the extent to give accurate stress results. Each of the eleven substructures would have to be modeled to include individual ring frames, beam flanges, plate stiffeners, etc. However, the Saturn I FEM <u>is</u> sufficient to make comparisons with the accuracy of the original analysis. Also, it contains enough detail to serve as a dynamic characteristics model.

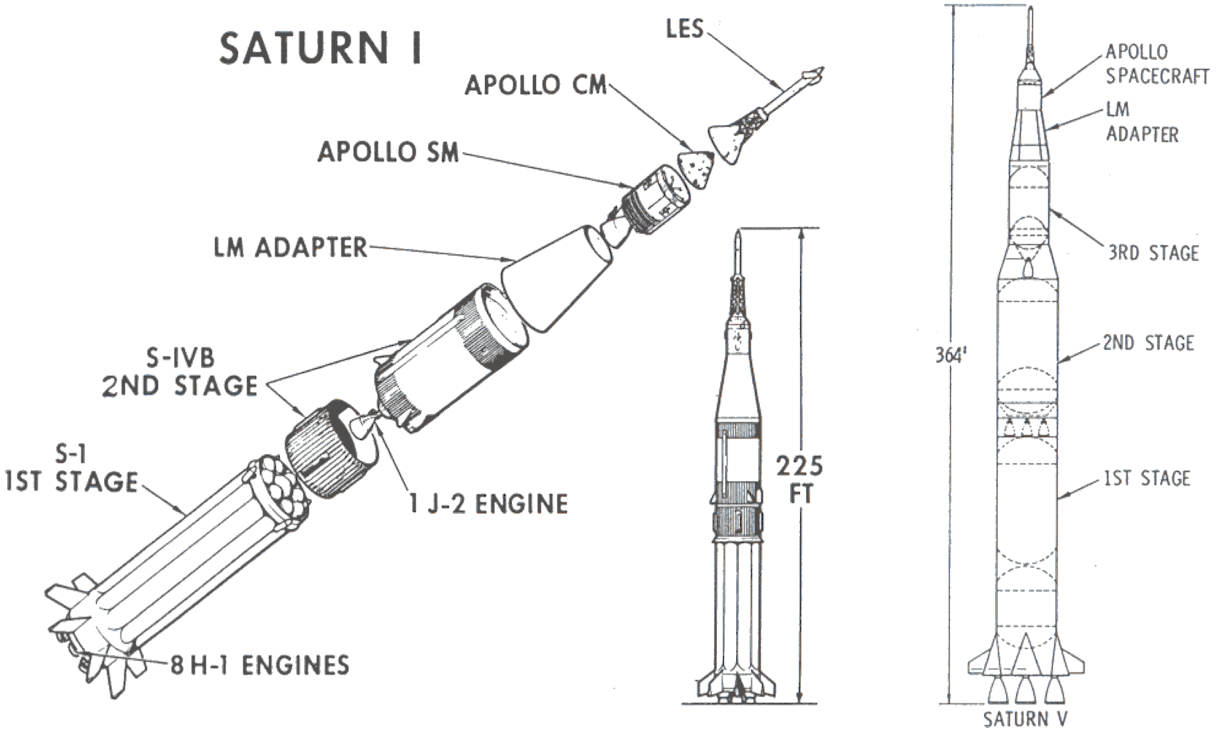

FIGURE 1: Saturn I and Saturn V Apollo Launch Vehicles

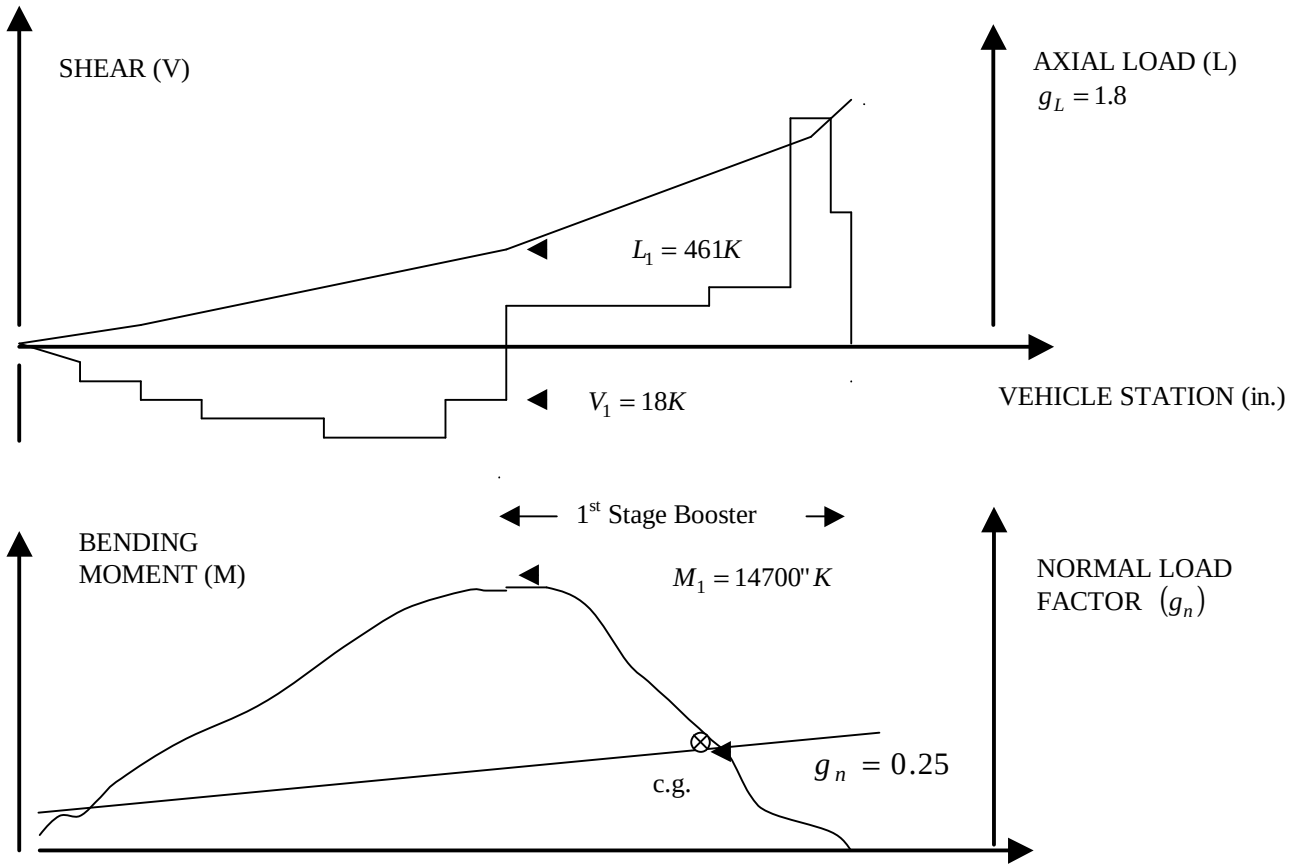

FIGURE 2: External Applied Launch Vehicle Loads

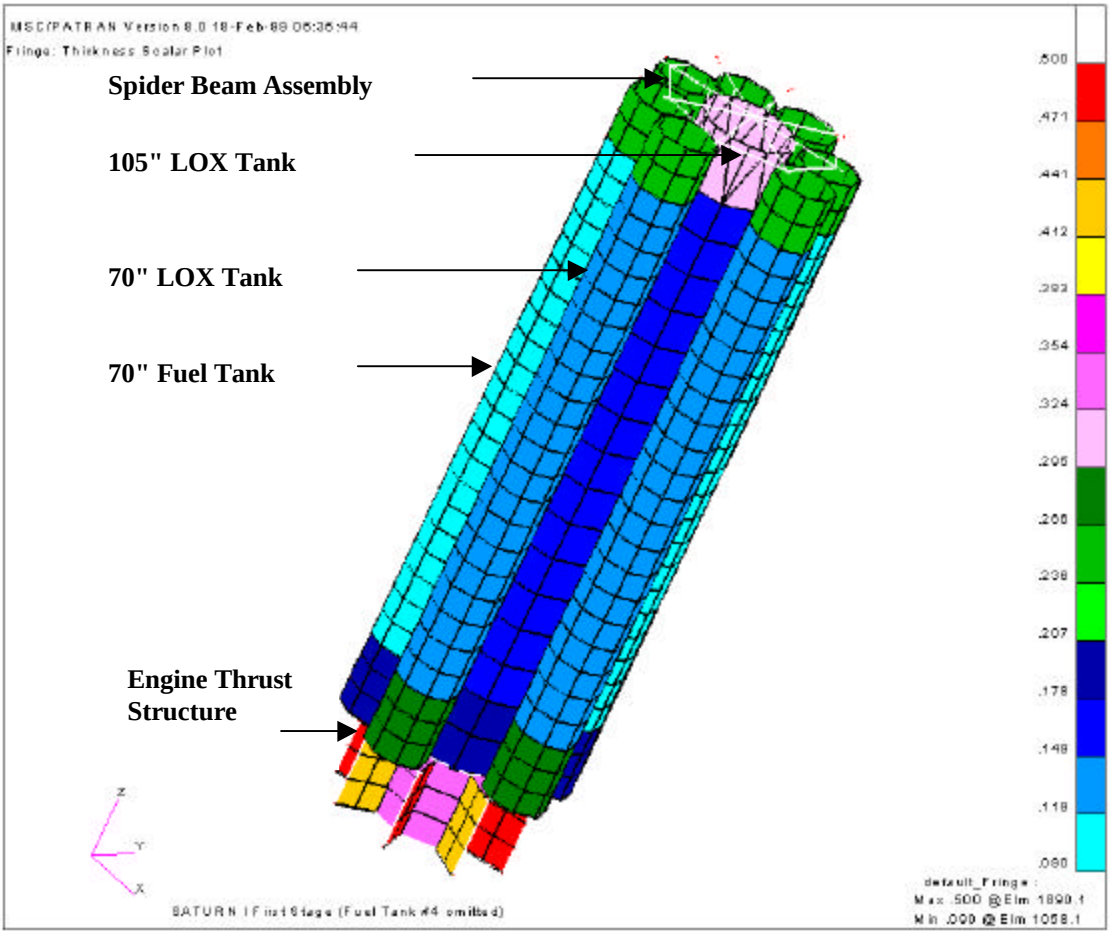

FIGURE 3: Saturn I First Stage Booster NASTRAN Finite Element Model

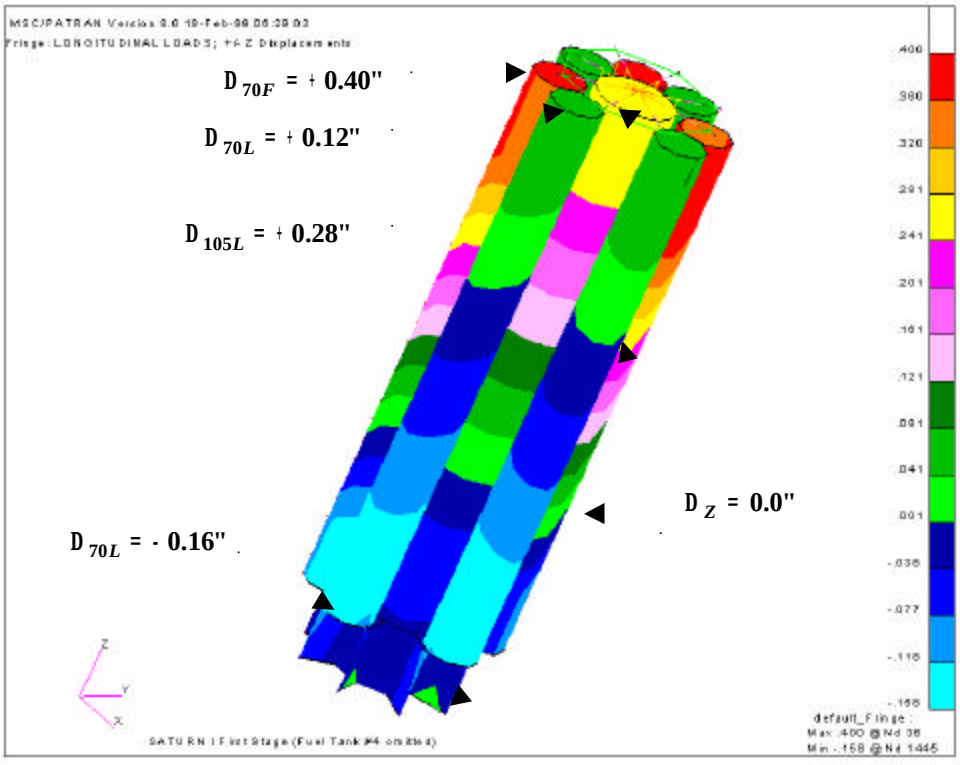

FIGURE 4: Saturn I FEM Results for Longitudinal Loads Analysis

Original Saturn I Internal Loads Analysis Approach

In the yesteryear, the Saturn booster internal loads distribution analysis was a "straight forward" application of the displacement (stiffness) method of analysis for statically indeterminate structures (Reference 1). This method involved the judicious selection of segmented free body cuts through the redundant booster structure to expose points (nodes) to which internal reaction forces were applied to achieve static equilibrium. The first free body cut chosen was at the interfaces between the spider beams and the outer 70" tanks (Figure 5). The cut included sixteen structural attachment pins with varying degrees of freedom associated with each of the pins.

Early on, it was obvious that the Saturn I loads distribution analysis would have to be performed in some sub-divided way to obtain satisfactory internal loads distributions. A separate longitudinal load distribution analysis and moment load distribution analysis had to be performed then superposed. The free body cut explained above was made for both longitudinal and moment loads analysis; however, different free body sub-divisions had to be made for each of the redundant equation formulations (Figures 6 & 7).

For pre-launch hold down and the one engine out external load conditions, a different and more complex set of free body and equation formulation had to be derived than for the all engine operating flight cases. A simple maximum Q all eight engine load set will be addressed in this paper. The goal is to present a gist of the tedious yesteryear structural analysis method performed versus the application of today's finite element techniques.

Symmetrical Free Body Considerations for Longitudinal Loads Analysis

Although initial free body cuts were made just below the spider beam assembly, the relationship of the inboard and outboard engines on the thrust structure below the 70" tanks also had to be considered in the displacement equation formulation. Figures 5 and 7 shows this relationship for a 70" LOX tank and fuel tank pair. For the longitudinal loads distribution analysis a set of six redundant internal reaction forces on the LOX tanks are exposed: $R_{A_1}, R_{A_2}, R_{B_1}, R_{B_2}, V_L$ and V_F.

Spider Beam Assembly Free Body Assumptions

Specific free body assumptions involving only the spider beam assembly were required to define the internal reaction forces on the inner 105" LOX tank. These assumptions that had to be made in order to keep the number of redundants to a minimum:

1. The longitudinal load for the spider beam free body segment (Figure 5) is reacted totally by the 70" LOX tank and 105" lox tank segment below, i.e. no shear load is transferred across the hub. The summation of forces static equilibrium expression defines the first longitudinal load analysis redundant equation, i.e.:

$$R_{A_1} + R_{A_2} + R_{B_1} + R_{B_2} = L/4 \qquad (1)$$

2. Torque load is not transmitted through the I-beam section to the hub of the assembly. The torsional stiffness of the open I cross-section is weak relative to the direct load path to the tanks below. This assumption defines the second redundant equation obtained by $\sum M_x = 0$, i.e.:

$$d_A \times R_{A_1} + d_B \times R_{A2} - d_a R_{B_1} - d_B R_{B_2} = 0 \qquad (2)$$

For each beam of the spider beam assembly free body, the deflection at the 70" LOX tank attachment pin (point 1) relative to the top of the 105" LOX tank (point 2) was defined by the application of the virtual-work method (Reference 1). This energy method was applied by using bending-moment diagrams drawn by cantilever parts (Table 1 and Figure 8). The following

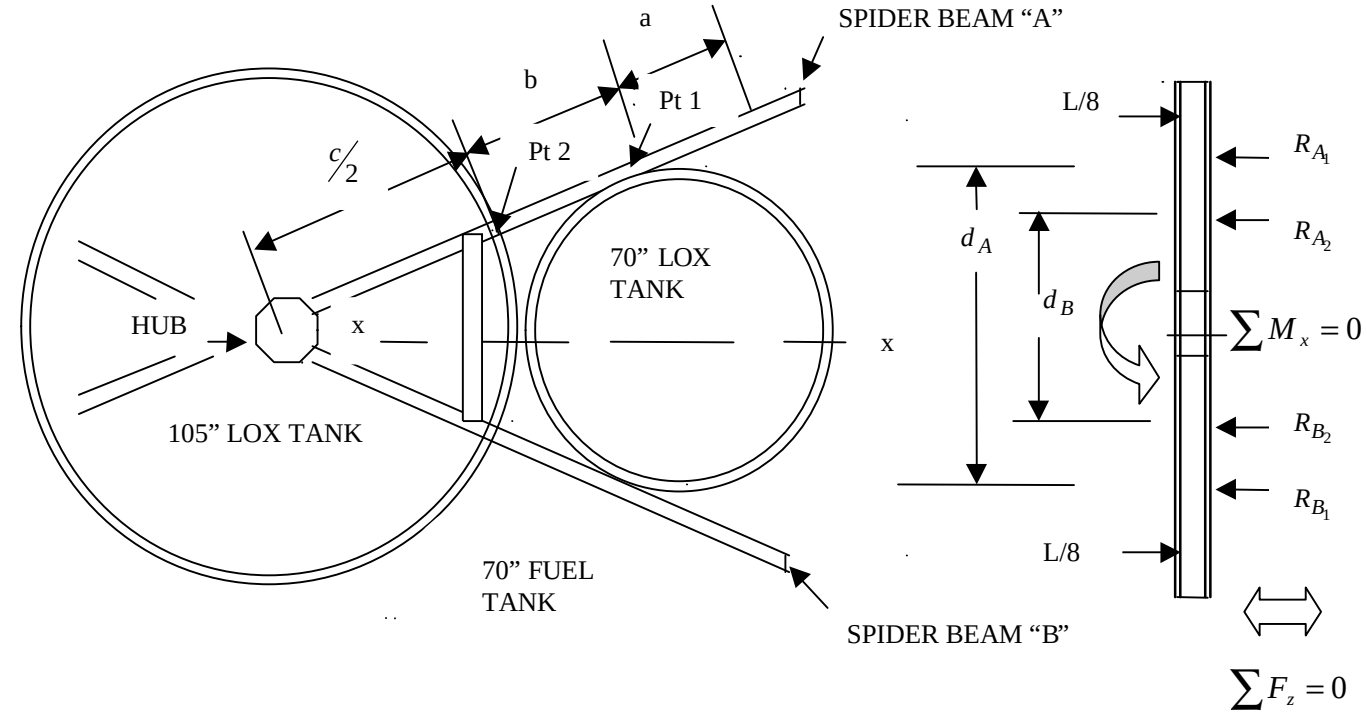

FIGURE 5: SPIDER BEAM FREEBODY OVER 105" TANK SEGMENT AND 70" LOX/FUEL TANK PAIR

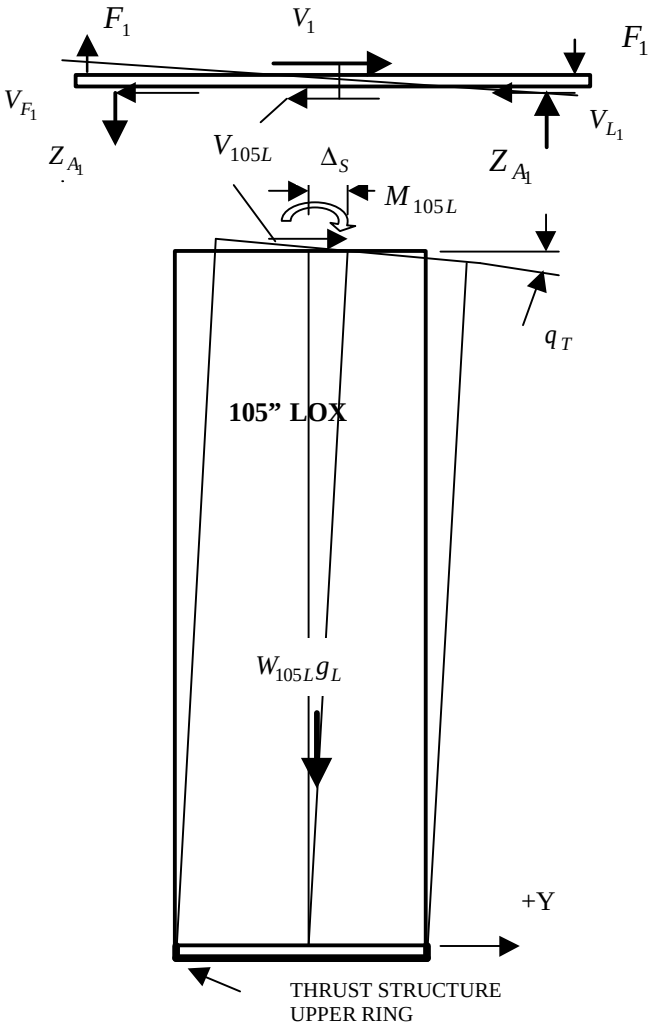

FIGURE 6: CENTER TANK/SPIDER BEAM IN BENDING

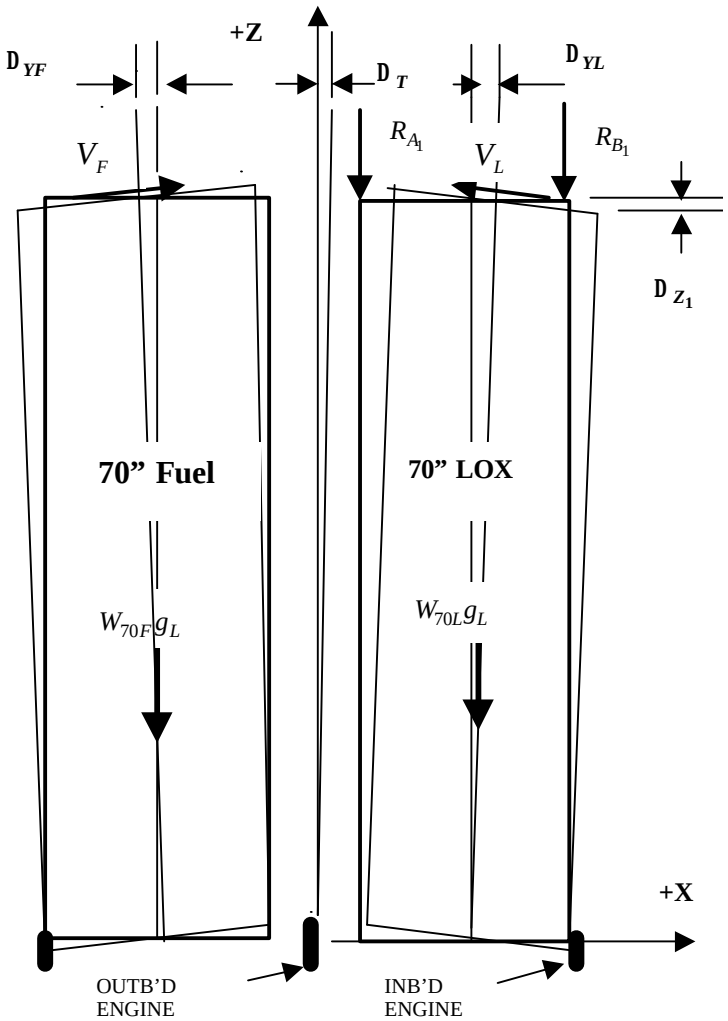

FIGURE 7: FREEBODY OF 70" LOX & FUEL TANK PAIR

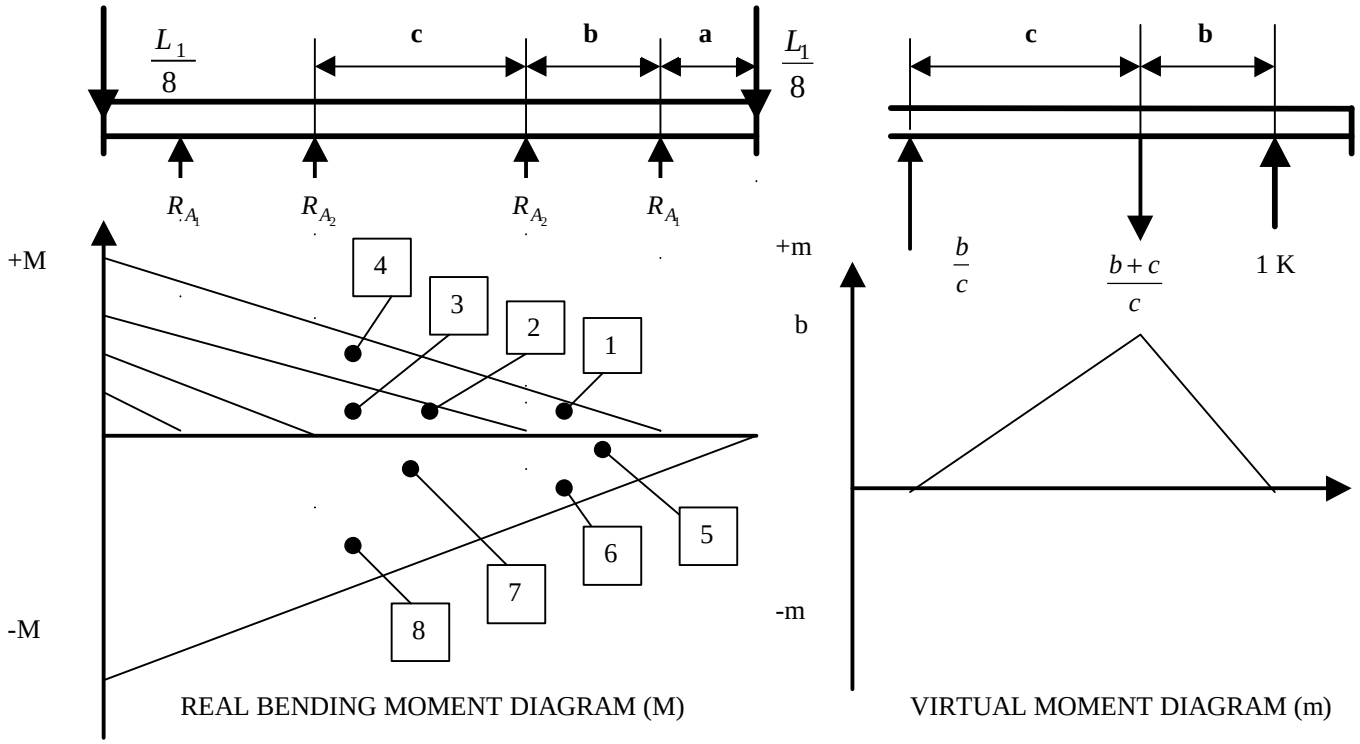

FIGURE 7: Spider Beam Bending Moment Diagrams by Cantilever Parts

TABLE 1: Spider Beam Real Moment and Unit Moment Components of Virtual Work

PART	REAL BENDING MOMENT (M)	UNIT (m)	VIRTUAL WORK COEFFICIENT (M m)
1	$\frac{b^2}{2}\cdot R_{A_1}$	$\frac{2}{3}b$	$\frac{b^3}{3}\cdot R_{A_1}$
2	$bc\cdot R_{A_1}$	$\frac{b}{2}$	$\frac{b^2c}{2}\cdot R_{A_1}$
3	$\frac{c^2}{2}\cdot R_{A_2}$	$\frac{b}{3}$	$\frac{bc^2}{6}\cdot R_{A_2}$
4	$\frac{c^2}{2}\cdot R_{A_1}$	$\frac{b}{3}$	$\frac{bc^2}{6}\cdot R_{A_1}$
5	$-ab\cdot\frac{L_1}{8}$	$\frac{b}{2}$	$-\frac{ab^2}{3}\cdot\frac{L_1}{8}$
6	$-\frac{b^2}{2}\cdot\frac{L_1}{8}$	$\frac{2}{3}b$	$-\frac{b^3}{3}\cdot\frac{L_1}{8}$
7	$-(a+b)\,c\cdot\frac{L_1}{8}$	$\frac{b}{2}$	$-\left[\frac{abc}{2}+\frac{b^2c}{2}\right]\cdot\frac{L_1}{8}$
8	$-\frac{c^2}{2}\cdot\frac{L_1}{8}$	$\frac{b}{3}$	$-\frac{bc^2}{6}\cdot\frac{L_1}{8}$
SUM	$\sum_1^8 M\cdot m$	$= \left[\frac{b^3}{3}+\frac{b^2c}{2}+\frac{bc^2}{6}\right]\cdot R_{A_1}+\left[\frac{bc^2}{6}\right]\cdot R_{A_2}-\left[\frac{ab^2}{2}+\frac{abc}{2}+\frac{b^2c}{2}+\frac{bc^2}{6}+\frac{b^3}{3}\right]\cdot\frac{L_1}{8}$	

combined equation for the vertical displacement of the spider beam "A" structural component was obtained:

$$\Delta_{B)R_A} = \left[\frac{b^3}{3} + \frac{b^2 c}{2} + \frac{bc^2}{6}\right] \times R_{A_1} + \left[\frac{bc^2}{6}\right] \times R_{A_2} - \left[\frac{ab^2}{2} + \frac{abc}{2} + \frac{b^2 c}{2} + \frac{bc^2}{6} + \frac{b^3}{3}\right] \times \frac{L_1}{8}$$

This component equation along with the component displacement expressions formulated below for the center 105" LOX tank, outer 70" tanks, and thrust structure were combined to define the coefficients of the final 6x6 stiffness matrix for the longitudinal loads analysis.

Center 105" Diameter LOX Tank Free Body

The center 105" LOX tank with upper and lower skirts was assumed the "grounded" free body. The bottom ring frame of the lower skirt (along with the upper ring frame of the thrust structure) was also assumed to be rigid in all degrees of freedom for all circumferential points (nodes). Any longitudinal deflection of the 105" tank will, of course, result in an equal longitudinal displacement of the entire spider beam assembly. Since we are interested only in one spider beam pair at a time, the vertical deflection of both points 1 and 2 of the spider beam (Figures 5 and 6) is given by:

$$\Delta_{B)R_c} = \left[\frac{8 l_{105L}}{\pi c t_{105e} E}\right] \left(\frac{R_{A_2} + R_{B_2}}{2}\right) = -K_{105L} \left(\frac{R_{A_2} + R_{B_2}}{2}\right)$$

The center 105" tank and; therefore, the spider beam deflections are also influenced by internal tank pressure, i.e.

$$\Delta_{B)_p} = \frac{c l_{105p}}{4 t_{105p} E} \times p_{105}$$

where l_{105p} = length between bulkheads

t_{105p} = thickness of pressurized length

p_{105} = pressure in 105" LOX tank

Outer 70" Diameter Tank Free Bodies

The outer 70" tank free bodies (Figure 7) were assumed to react the internal redundant loads as a simple beam from top to bottom, analogous to a NASTRAN BEAM finite element. The load bearing 70" LOX tanks have vertical and lateral displacements at the top, which are given by simple beam formula as:

$$\Delta_{R_1} = \left[\frac{d^2 l_{70L}}{8 E I_{70L}}\right] \times R_{A_1} - \left[\frac{d^2 l_{70L}}{8 E I_{70L}}\right] \times R_{B_1} + \left[\frac{d l_{70L}^2}{12 E I_{70L}}\right] \times V_L$$

$$\Delta_{YL} = \left[\frac{l_{70L}^3}{3 E I_{70L}}\right] \times V_L$$

Also for the 70" fuel tank; which does not react longitudinal forces at the top, the lateral displacement is given by:

$$\Delta_{YF} = \left[\frac{l_{70F}^3}{3 E I_{70F}}\right] \times V_F$$

The 70" LOX (and fuel) tank displacement is also impacted by internal pressure, i.e.:

$$\Delta R)_p = \frac{dl_{70L}}{4t_{70p}E} \times p_{70L}$$

Note that in the free body schematic shown in Figure 7; an allowance has been made for a tangential displacement (Δ_T) at the top of the tanks. This is due to the differential thrust structure displacement below resulting from the inboard and outboard engine placements. Also the alternately placed 70" LOX and fuel tanks have different bending stiffness, thus a resultant torque force $(V_L - V_F)$ is applied to the center 105" LOX tank. Therefore, the following equation for tangential deflection must be considered in the subsequent formulation:

$$\Delta_T = \frac{2\left[b + \left(\frac{c}{2}\right)^2\right] l_{105L}}{p\left(\frac{c}{2}\right)^3 t_{105e}G} \times (V_L - V_F)$$

Thrust Structure Free Body

The upper ring frame of the thrust structure was considered "grounded" in all six degrees of freedom. The following spring constant expressions were defined for the deflections at the 70" tank upper attach points due to the relative displacements below:

$$\Delta R)_A = - K_{OE} \times R_{AB} + K_{OT} \times T_V$$

$$\Delta R)_B = - K_{IE} \times R_{BB}$$

where

$$R_{AB} = R_{A_1} + \frac{l_{70L}}{d} \times V_L + \frac{W_{70L}}{2} \times g_L$$

$$R_{BB} = R_{B_1} - \frac{l_{70L}}{d} \times V_L + \frac{W_{70L}}{2} \times g_L$$

and K_{OE}, K_{OT} and K_{IE} were determined from static tests. (See Figure 10)

Displacement Compatibility at Free body Segment Cuts

Sufficient deflection definition is now formulated for each structural "finite" element to write equations, which equate the spider beam vertical displacements (point 1) to the 70" LOX tank upper attachment pin displacements. For the spider beam "A" free body (Figure 5), a position above an outboard engine, the following displacement relationship can be defined for the third redundant equation:

$$\Delta B)_{R_A} + \Delta B)_{R_c} + \Delta B)_p = \Delta R_1 + \Delta R)_p + \Delta R)_A \qquad (3)$$

For spider beam "B" positioned above an inboard engine, the following relationship is valid for the fourth redundant equation:

$$\Delta B)_{R_B} + \Delta B)_{R_c} + \Delta B)_p = - \Delta R_1 + \Delta R)_p + \Delta R)_B \qquad (4)$$

An example of the full-expanded form of displacement Equation 3 is presented in Figure 8.

Two additional redundant equations, which equate spider beam lateral displacements to the 70" LOX (and fuel) tank attachment pins, completes the 6x6 "stiffness matrix" formulation. These two displacement equations are, in simplest terms:

$$\Delta_{YL} + \Delta_T = \theta_R l_{70L} \tag{5}$$

$$\Delta_{YF} - \Delta_T = \theta_R l_{70F} \tag{6}$$

where $\theta_R = \frac{1}{d_A}\left[\left(\Delta_R\right)_A - \Delta_R\right)_B\right]$

$$\Delta_B)_{R_A} + \Delta_B)_{R_C} + \Delta_B)_p = \Delta_{R_1} + \Delta_R)_p + \Delta_R)_A \tag{3}$$

$$\left[\frac{1}{EI_B}\left(\frac{b^3}{3} + \frac{b^2c}{2} + \frac{bc^2}{6}\right) + \frac{l_{70L}c^2}{8EI_{70L}} + \frac{b}{A_BG} + \frac{K_{70L}}{2}\right] \times R_{A_1} + \left[\frac{K_{70L}}{2} - \frac{l_{70L}c^2}{8EI_{70L}} + \frac{B_{BV}}{2}\right] \times R_{B_1}$$

$$+ \left[\frac{bc^2}{6EI_B} - \frac{K_{105L}}{2}\right] \times R_{A_2} - \left[\frac{K_{105L}}{2}\right] \times R_{B_2} + \left[\frac{l_{70L}{}^2c}{12EI_{70L}}\right] \times V_L$$

$$= \left[\frac{L_1 g_L}{8EI_B}\left(\frac{ab^2}{2} + \frac{abc}{2} + \frac{bc^2}{6} + \frac{b^3}{3}\right) + \frac{L_1 g_L b}{8A_BG} + \frac{W_{105L}g_L}{pcE}\left(\frac{l_{105s}}{t_{105s}}\right) - \frac{W_{70L}g_L}{pdE}\left(\frac{l_{70s}}{t_{70s}}\right)\right.$$

$$\left. - \frac{P_{105}cl_{105p}}{4Et_{105p}} + \frac{P_{70}dl_{70p}}{4Et_{70p}} + \frac{a}{2}l_{70L}\right] \times \Delta T + T_{E_v}B_{E_v}$$

FIGURE 8: Longitudinal Loads Analysis Equation # 3

$$\Delta_B)_{Z_{A_1}} + \left(b + \frac{c}{2}\right) \times \theta_{T_{105L}} = \Delta_{70L})_{Z_{A_1}} \tag{7}$$

$$\left[\frac{1}{EI_B}\left(\frac{b^3}{3} + \frac{b^2c}{6}\right) + \frac{b}{A_BG} + \frac{(2b+c)^2 l_{70L}}{2EI_{105L}} + \frac{l_{70L}d^2}{8EI_{70L}} + \frac{K_{70L}}{2} + \frac{B_{BV}}{2}\right] \times Z_{A_1}$$

$$+ \left[\frac{.707(2b+c)^2 l_{70L}}{2EI_{105L}} - \frac{l_{70L}c^2}{8EI_{70L}} + \frac{K_{70L}}{2} + \frac{B_{BV}}{2}\right] \times Z_{B_1} + \left[\frac{.707(2b+c)^2 l_{70L}}{2EI_{105L}}\right] \times Z_{B_2}$$

$$+ \left[\left(\frac{(2b+c)l_{70L}{}^2}{2EI_{105L}}\right)\sin 22.5 + \frac{l_{70L}{}^2c}{12EI_{70L}}\right] \times V_{L_1} + \left[\left(\frac{(2b+c)l_{70L}{}^2}{2EI_{105L}}\right)\cos 22.5\right] \times V_{L_2}$$

$$+ \left[\left(\frac{(2b+c)l_{70F}{}^2}{2EI_{105L}}\right)\sin 22.5 + \frac{l_{70L}B_{BV}}{2d}\right] \times V_{F_1} + \left[\left(\frac{(2b+c)l_{70F}{}^2}{2EI_{105L}}\right)\cos 22.5 + \frac{l_{70F}B_{BV}}{2d}\right] \times V_{F_2}$$

$$= \left[\frac{1}{EI_B}\left(\frac{b^3}{3} + \frac{b^2c}{6} + \frac{ab^2}{2} + \frac{abc}{6}\right) + \frac{b}{A_BG}\right] \times F_1$$

$$- \left[\frac{(2b+c)l_{70L}}{EI_{105L}}\left(W_{70L}l_{70Lz} + W_{70F}l_{70Fz}\right) + \frac{(2b+c)W_{105L}l_{105Lz}{}^2}{4EI_{105L}} + \frac{l_{70Lz}d}{12EI_{70L}}\left(\frac{l_{70L}{}^2 - l_{70Lz}{}^2}{l_{70L}}\right)W_{70L}\sin 22.5\right] \times g_n$$

FIGURE 9: Moment Loads Analysis Displacement Equation # 7

FIGURE 10: Original Saturn I Structural Test Set-up Sketches

At the time of the original Saturn I internal loads analysis, a one engine out condition was also considered for which six additional longitudinal displacement expressions had to be formulated that required a 12x12 matrix solution. The six additional redundants were for internal loads over and adjacent to the engine out position. This formulation is not presented in this paper.

Symmetrical Free Body Redundants for Moment Loads Analysis

For the moment loads analysis a free body subdivision involving only the "grounded" center 105" LOX tank and spider beam assembly had to be first considered (Figure 5). The 105" tank was assumed to react to all internal loads as a simple beam resulting in an angular deflection (slope) of the spider beam assembly relative to the rigid lower 105" ring frame. Bending of the 105" tank and spider beam assembly is due to two sets of loads applied to the free body:

1. The applied external loads M_1 and V_1 above the spider beam. The external moment M_1 was applied to the spider beam as equivalent two force couples F_1 and $F_2 = .707 \cdot F_1$.
2. The internal moment redundant forces $Z_{A_1}, Z_{B_1}, Z_{A_2}, Z_{B_2}, V_{L_1}, V_{L_2}, V_{F_1}$ and V_{F_2}; which arise from the resistance (to bending) of the 70" LOX (and fuel) tanks. These internal loads were defined at the same 70" tank attachment pin locations as in the longitudinal load analysis.

Spider Beam Assembly Displacements due to Moment Loads

The virtual-work method was also applied to obtain spider beam displacements as a function of external moment loads and internal redundant forces, i.e.:

$$\Delta_B)_{Z_A} = \left[\frac{b^3}{3} + \frac{b^2 c}{6}\right] \times Z_{A_1} - \left[\frac{abc}{6} + \frac{ab^2}{2} + \frac{b^3}{3} + \frac{b^2 c}{6}\right] \times F_1$$

From symmetry it is evident that the deflections at each end of the beam are the same, but opposite in sign; therefore, in the formulation, only the displacements on one side of the neutral axis are considered. The overall lateral displacement (Δ_S) and slope (Θ_T) of the spider beam assembly are given by:

$$\Delta_{S_{105L}} = \frac{l_{105L} M_{105T}}{2EI_{105L}} + \frac{l_{105L} \times V_{105T}}{3EI_{105L}}$$

and

$$\Theta_{T_{105L}} = \frac{l_{105L} \times M_{105T}}{EI_{105L}} + \frac{l^2_{105L} \times V_{105T}}{2EI_{105L}}$$

Outer 70" Diameter Tank Free Bodies for Moment Loads

The moment redundant forces will either compress or elongate (and bend) any particular 70" tank depending upon which side of the neutral axis is being considered. For a given 70" LOX and fuel tank pair, the same general displacement expressions as for the longitudinal load distribution apply, i.e. for 70" LOX tank:

$$\Delta_{70L})_Z = \left[\frac{d^2 l_{70L}}{8EI_{70L}}\right] \times Z_{A_1} - \left[\frac{d^2 l_{70L}}{8EI_{70L}}\right] \times Z_{B_1} + \left[\frac{d l^2_{70L}}{12EI_{70L}}\right] \times V_{LZ_1}$$

$$\Delta_{YL})_Z = \left[\frac{l_{70L}}{3EI_{70L}}\right] \times V_{LZ_1}$$

Similar displacements for a second 70" LOX tank and fuel tank pair must be considered to complete the definition of one full side of the neutral axis of bending. Additional displacements due to the moment redundant loads on the thrust structure must also be considered.

Displacement Compatibility for Moment and Lateral Load

Again, as in the longitudinal loads analysis, expressions which equate spider beam displacements to 70" tank displacements for the external moment loading conditions can be written. There exist eight (8) unknown internal moment redundants $Z_{A_1}, Z_{B_1}, Z_{A_2}, Z_{B_2}, V_{L_1}, V_{L_2}, V_{F_1}$ and V_{F_2}.

Consideration of both vertical and lateral displacements at each of four 70" LOX tank attachment pin locations (on one side of the neutral axis) will allow eight simultaneous displacement equations to be written. These equations in simplified form are given below. Example of the full-expanded form of the spider beam "A" displacement equation is given in Figure 9.

$$\Delta_B)_{Z_{A_1}} + \left(b + \frac{C}{2}\right)\theta_{T_{105L}} = \Delta_{70L})_{Z_{A_1}} \tag{7}$$

$$\Delta_B)_{Z_{B_1}} + 0.707\left(b + \frac{C}{2}\right)\theta_{T_{105L}} = \Delta_{70L})_{Z_{B_1}} \tag{8}$$

$$\Delta_{Z_{B_2}}) + 0.707\left(b + \frac{C}{2}\right)\theta_{T_{105L}} = \Delta_{70L})_{Z_{B_2}} \tag{9}$$

$$\Delta_B)_{Z_{A_2}} = \Delta_{70L})_{Z_{A_2}} \tag{10}$$

$$\Delta_{YL})_{Z_1} - \Delta_{S_{105L}} \cos 22.5^0 = l_{70L}\theta_{70L_1} \tag{11}$$

$$\Delta_{YL})_{Z_2} - \Delta_{S_{105L}} \sin 22.5^0 = l_{70L}\theta_{70L_2} \tag{12}$$

$$\Delta_{YF})_{Z_1} - \Delta_{S_{105L}} \sin 22.5^0 = l_{70F}\theta_{70F_1} \tag{13}$$

$$\Delta_{YF})_{Z_2} - \Delta_{S_{105L}} \cos 22.5^0 = l_{70F}\theta_{70F_2} \tag{14}$$

Combined Longitudinal and Moment Loads

Both longitudinal load and moment load analyses were resolved and combined by a FORTRAN computer program. The complete flight load case results were documented (Reference 2) and presented in a free body form as shown in Figure 11. Note that the original longitudinal loads analysis distribution is also presented and compared to the NASTRAN FEM element force output at the spider beam and propellant tank interface. Differences are attributed to unknown thrust structure spring constant values that had to be estimated for the FEM construction.

The accuracy of the original internal loads analysis was tested by a short tank test (Figure 10) at MSFC. Local relative displacement data was recorded and, where required, some of the spring constant values used in the analysis were updated. The analysis was also verified by on-board Saturn I flight strain gauge data.

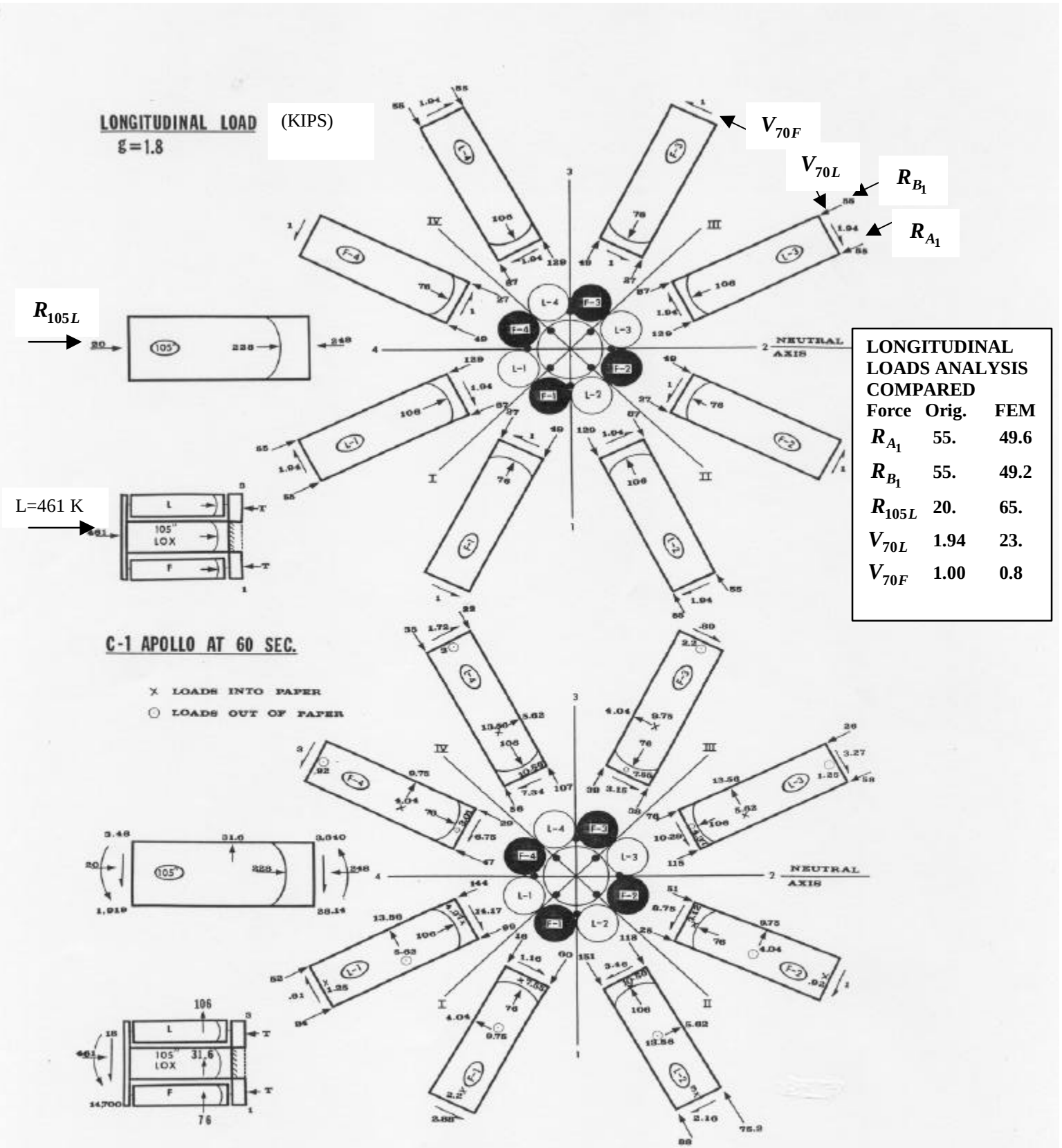

FIGURE 11: Original Saturn I Internal Loads Distribution Analysis Results

Saturn I Stress and Dynamic Analysis Usage

The internal loads distribution analysis results were used by the various stress and dynamics analysis groups in the NASA/MSFC organization at the time. Typical analysis groups were the propellant tank stress group, tail section stress group, interface structures group, and vehicle flight dynamics group. Stress analyses were made via classical hand calculation methods (References 3 & 4). However, due to the fast development phase of the Saturn program, most of the overall structural verification was based on the numerous structural static and dynamic tests that were performed at MSFC during that period. Today, most of the structural testing is surrogated by the "virtual reality" type finite element modeling techniques available via MSC NASTRAN/PATRAN software products.

Conclusions

This paper attempts to demonstrate, by direct comparison, the degree and volume of academic "dog" work that is circumvented by the application of currently available structural analysis programs, i.e. MSC/NASTRAN. The finite element method has been used for over thirty years and is now the backbone of rigorous structural analysis and allows today's engineers to be more professionally empowered.

Trademark Acknowledgments

References

1. Popov, E. P. *Mechanics of Materials*, Prentice-Hall, 1958
2. Gamblin, C. R. *Saturn S-I Stage Internal Loads Distributions*, NASA/MSFC Internal Note P&VE-S-63-9, Huntsville, AL, August 1, 1963.
3. Perry, David J. *Aircraft Structures*, McGraw-Hill, 1950
4. Roark, R. J. *Formulas for Stress and Strain*,3rd McGraw-Hill, 1954

Glossary of Terms

EI	Elastic Modulus and Moment of Inertia Product
FEM	Finite Element Model
G	Elastic Shear Modulus
LOX	Liquid Oxidizer
MSC	MacNeal-Schwendler Corporation
MSFC	Marshall Space Flight Center
NASA	National Aeronautics and Space Administration
Q	Dynamic Pressure Load Factor